# NiO Junction Termination Extension for Ga<sub>2</sub>O<sub>3</sub> Devices: High Blocking Field, Low Capacitance, and Fast Switching Speed

Ming Xiao\*,#, Boyan Wang\*,#, Ruizhe Zhang\*, Qihao Song\*, Joseph Spencer\*,+, Zhonghao DuΨ, Yuan Qin\*, Kohei Sasaki<sup>ξ</sup>, Han WangΨ, Marko Tadjer+, and Yuhao Zhang\*

\*These two authors contributed equally to this work. Email: {mxiao, yhzhang}@vt.edu

\*Center for Power Electronics Systems, Virginia Tech, Blacksburg, USA

\*U.S. Naval Research Laboratory, Washington DC, USA

\*Department of Electrical and Computer Engineering, University of Southern California, Los Angeles, USA

\*Novel Crystal Technology, Inc., Saitama, Japan

Abstract—This work investigates the blocking electric field, capacitance, and switching speed of the p-type NiO based junction termination extension (JTE) for vertical Ga<sub>2</sub>O<sub>3</sub> devices. The JTE comprises multiple NiO layers sputtered on the surface of Ga<sub>2</sub>O<sub>3</sub> drift region, the acceptor concentration and length of which are carefully optimized. This NiO JTE enabled a breakdown voltage over 3 kV in vertical Ga<sub>2</sub>O<sub>3</sub> diodes with a parallel-plate junction field of 4.2 MV/cm. Large-area Ga<sub>2</sub>O<sub>3</sub> p-n diodes with a current over 1 A were fabricated to evaluate the JTE's capacitance and switching characteristics. The JTE accounts for only ~11% of the junction capacitance of this 1 A diode, and the percentage is expected to be even smaller for higher-current diodes. The turn-ON/OFF speed and reverse recovery time of the diode are comparable to commercial SiC Schottky barrier diodes. These results show the good promise of NiO JTE as an effective edge termination for Ga<sub>2</sub>O<sub>3</sub> power devices.

Keywords—ultra-wide bandgap, gallium oxide, nickel oxide, junction termination extension, reverse recovery, switching tests

# I. INTRODUCTION

The advances in power semiconductor devices rely on the combined innovations in semiconductor materials and device architectures [1]. Gallium oxide (Ga<sub>2</sub>O<sub>3</sub>) is a promising ultrawide bandgap (UWBG) material for power devices due to its high critical electric field, controllable doping, and availability of large-diameter wafers [2], [3]. Up to now, Ga<sub>2</sub>O<sub>3</sub> is the only UWBG material that has met several key milestones for power semiconductor development, including the 6-inch wafer, high-current (>100 A) device, packaging, electrothermal ruggedness, and converter applications [4], [5].

A critical challenge for Ga<sub>2</sub>O<sub>3</sub> power devices is the lack of p-type doping in Ga<sub>2</sub>O<sub>3</sub>, which, in particular, makes the edge termination design very difficult. Prior Ga<sub>2</sub>O<sub>3</sub> edge terminations mainly rely on the field plate [6], implantation [7], and trench structures [8]. Recently, an alternative WBG p-type material, nickel oxide (NiO), is found to be able to form high-quality hetero-PN junction with Ga<sub>2</sub>O<sub>3</sub> [9], [10] and GaN [11], [12].

This work was supported in part by National Science Foundation under Grants ECCS-2100504 and ECCS-2230412 and in part by the Center for Power Electronics Systems High Density Integration Industry Consortium.

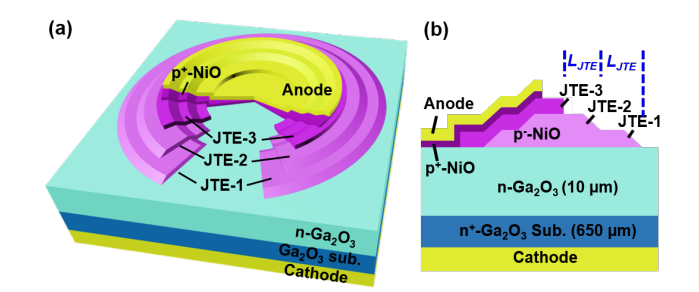


Fig. 1. (a) 3-D schematic of the Ga<sub>2</sub>O<sub>3</sub> PND with NiO JTE (part of the anode, p<sup>+</sup>-NiO and JTEs are removed to show the internal device structure). (b) Schematic of the JTE region.

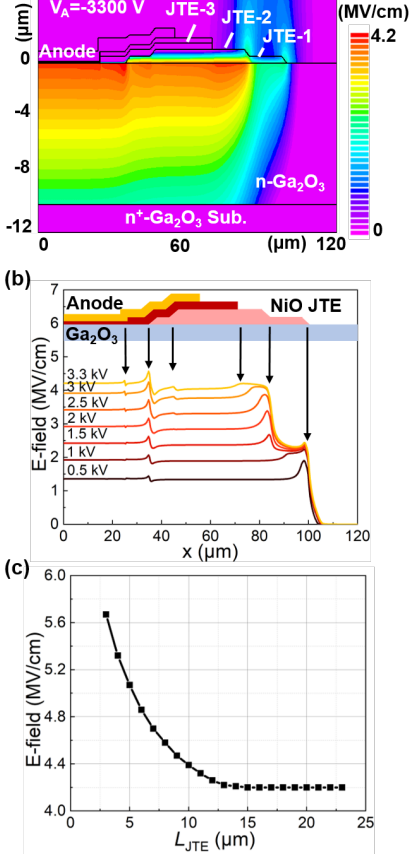
NiO has also been used to form a single-zone junction termination extension (JTE) for Ga<sub>2</sub>O<sub>3</sub> devices [13]. However, the effectiveness of the single-zone JTE is known to be sensitive to the charge density.

Recently, we proposed a multi-layer NiO JTE, in which the lengths of NiO layers decrease from the bottom towards the top to enable a graded decrease in charge density away from the device active area [14], [15]. This NiO JTE has broad design window, large process latitude, and high effectiveness. It has been applied to vertical Ga<sub>2</sub>O<sub>3</sub> Schottky barrier diodes (SBDs) [14] and p-n diodes [15] to achieve the multi-kilovolt breakdown voltage (*BV*).

This work extends our prior works into evaluating the blocking electric field (E-field), capacitance, and switching characteristics of the graded NiO JTE technology. Low parasitic capacitance and high switching speed are critical requirement for any edge terminations of power devices. However, such studies have not been reported in Ga<sub>2</sub>O<sub>3</sub> devices. This work fills this gap by fabricating large-area NiO/Ga<sub>2</sub>O<sub>3</sub> p-n diodes with the graded NiO JTE to evaluate the JTE's characteristics. A double-pulse test (DPT) setup for on-wafer devices is developed for testing the switching characteristics of the JTE p-n diode (PND).

### II. JTE DESIGN AND FABRICATION

The NiO JTE comprises two layers of p-NiO (JTE-1 and -2) and one layer of p-NiO (JTE-3) sputtered on the surface of



E-field

(a)

Fig. 2. (a) Simulated E-field contour in the PND at a reverse bias of 3.3 kV. (b) The E-field profile in  $Ga_2O_3$  at the PND blocking voltage increased from 0.5 to 3.3 kV. (c) The simulated junction field at 3.3 kV as a function of  $L_{\rm JTE}$ .

the Ga<sub>2</sub>O<sub>3</sub> drift region (Fig. 1). An p<sup>+</sup>-NiO is sputtered below the anode to enable low p-layer resistance in the PND active region. The thickness and acceptor concentration ( $N_{\rm A}$ ) of p<sup>-</sup>-NiO, p-NiO and p<sup>+</sup>-NiO layers are 400 nm and ~3×10<sup>17</sup> cm<sup>-3</sup>, 350 nm and ~10<sup>18</sup> cm<sup>-3</sup>, and 250 nm and >10<sup>19</sup> cm<sup>-3</sup>, respectively. The  $N_{\rm A}$  of NiO is controlled by modulating the Ar/O<sub>2</sub> gas ratio in the sputtering process, as elaborated in our prior work [12]. The two p<sup>-</sup>-NiO layers are designed to be fully depleted at the device BV. Hence, their total thickness ( $t_{\rm NiO}$ ) can be roughly determined according to  $t_{NiO}N_A\approx E_M\varepsilon_{GaO}$ , where  $E_M$  is the junction field in Ga<sub>2</sub>O<sub>3</sub> at BV and  $\varepsilon_{GaO}$  is the Ga<sub>2</sub>O<sub>3</sub>'s permittivity [14].

The detailed simulations on the JTE's design space, tradeoff, and design window are illustrated in [15]. Fig. 2(a)-(b) show the simulated E-field contour in the p-n diode at the increased reverse bias up to 3.3 kV. The E-field crowding is effectively suppressed. Fig. 2(c) show the peak E-field as a function of the incremental JTE length ( $L_{\rm JTE}$ ), revealing a saturation effect in the peak E-field decrease as  $L_{\rm JTE}$  increases.

The wafer used in this work is the 2-inch  $Ga_2O_3$  wafer with a drift region thickness of  $10~\mu m$  and a net donor concentration of  $1.3\times10^{16}~cm^{-3}$ . Fig. 3(a) shows the main device fabrication steps. The fabrication starts with the cathode Ohmic contact formation, followed by the sputtering and lift-off of two p<sup>-</sup>-NiO

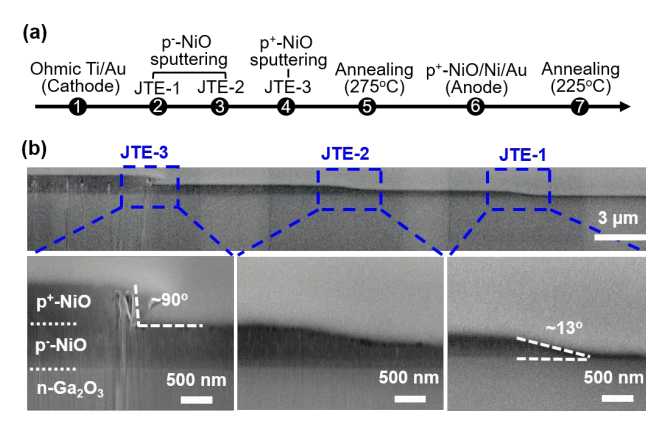


Fig. 3. (a) Main fabrication steps of the Ga<sub>2</sub>O<sub>3</sub> JTE-PND. (b) Cross-sectional SEM images of the entire and each JTE region of the fabricated NiO/Ga<sub>2</sub>O<sub>3</sub> PND.

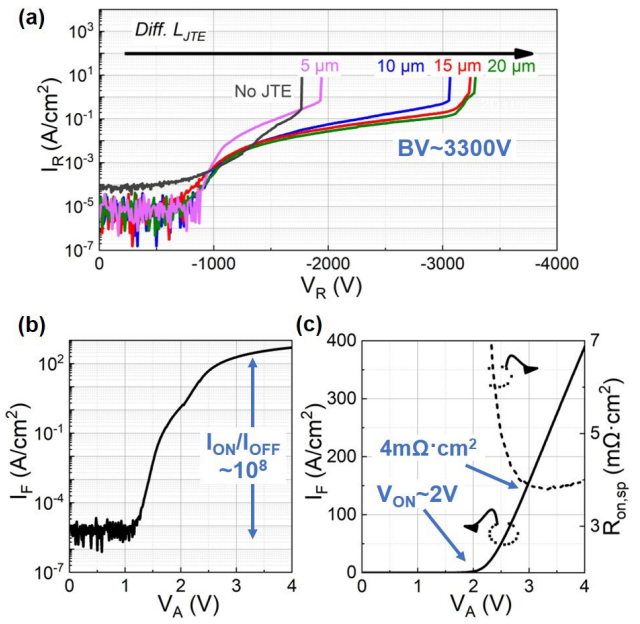


Fig. 4. (a) Reverse I-V characteristics of the PNDs without the JTE and the JTE-PNDs with different  $L_{\rm JTE}$  of 5, 10, 15, and 20  $\mu$ m. Forward I-V characteristics in (b) semi-log and (c) linear scales.

JTE layers and a p<sup>+</sup>-NiO JTE layer. After a post-sputter annealing, the p<sup>+</sup>-NiO anode layer and Ni/Au Ohmic contact are deposited, followed by a final annealing. Fig. 3(b) shows the cross-sectional SEM image of the fabricated JTE region.

### III. STATIC AND SWITCHING CHARACTERISTICS

Fig. 4 shows the characteristics of the fabricated p-n diodes with JTE (JTE-PNDs), revealing a BV up to 3.3 kV and a differential specific on-resistance ( $R_{\rm ON,SP}$ ) of 4 m $\Omega$ ·cm<sup>2</sup>. Fig. 5 (a)-(b) show the characteristics of the large-area JTE-PNDs with a forward current >1 A. Fig. 5(c) shows the C-V characteristics of the large-area JTE-PNDs. The capacitance associated with the JTE region is calculated by subtracting the active-area junction capacitance from the measured capacitance. Note that this calculation can overestimate the JTE-related capacitance, as it also accounts for the diffusion capacitance and other parasitics.

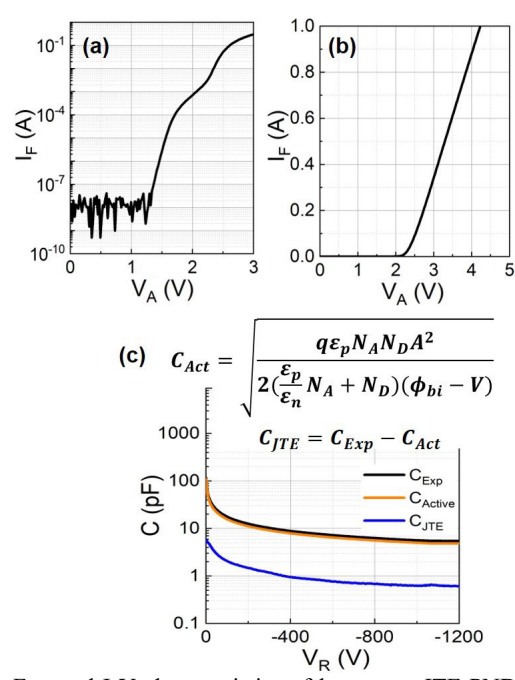


Fig. 5. Forward I-V characteristics of large-area JTE-PNDs in (a) semi-log and (b) linear scales. (c) C-V characteristics and the model to separate the active-region capacitance ( $C_{Act}$ ) and JTE region capacitance ( $C_{ITE}$ ) in the total experimental capacitance ( $C_{Exp}$ ).  $N_D$  and  $N_A$  are the net donor/acceptor concentration in Ga<sub>2</sub>O<sub>3</sub> and NiO.  $\varepsilon_n$  and  $\varepsilon_p$  is the permittivity of Ga<sub>2</sub>O<sub>3</sub> and NiO, respectively.  $\Phi_{bi}$  is the built-in potential of the NiO/Ga<sub>2</sub>O<sub>3</sub> hetero-junction.

Under this overestimation scenario, JTE capacitance accounts for only ~11% of the device capacitance. This percentage is expected to continuously decrease in devices with larger current ratings, as the main area capacitance scales with the device area while the JTE capacitance scales with the device perimeter.

The switching characteristics of the JTE-PNDs are measured by a custom DPT setup for on-wafer device characterizations. As shown in Fig. 6(a)-(c), the setup connects a DPT board with the probe. This switching test setup obviates the need for device packaging at the price of higher circuit parasitics (from the probe-board connection) than the full board-level circuit test.

Fig. 6(d)-(e) shows the 3A/800V turn-OFF/ON waveforms of the  $Ga_2O_3$  JTE-PNDs and a commercial SiC SBD (IDH02G120C5). The  $Ga_2O_3$  JTE-PNDs show a reverse recovery time of 43 ns and the rise/fall time of  $\sim 12/14$  ns, both being similar to the SiC SBD tested under the same setup. This suggests the NiO JTE does not limit the switching speed of  $Ga_2O_3$  devices.

# IV. BENCHMARK AND SUMMARY

Fig. 7 benchmarks the *BV vs.* differential- $R_{\rm ON,SP}$  of our JTE-PND with other  $\rm Ga_2O_3$  diodes. Thanks to the effectiveness of the JTE, the performance of our JTE-PND is comparable to the state-of-the-art  $\rm Ga_2O_3$  diodes. Table I compares our graded NiO JTE with the representative reports of other termination technologies for  $\rm Ga_2O_3$  devices, including the combinations of implantation and field plate (FP) [7], trench and FP [8], as well as high-k dielectric FP [16]. Our graded NiO JTE features the concurrent realization of high parallel-plate junction E-field of 4.2 MV/cm, low parasitic capacitance, and fast switching speed.

In summary, this work presents comprehensive studies of the static and switching characteristics of a new NiO-based JTE for vertical Ga<sub>2</sub>O<sub>3</sub> devices. Large-area Ga<sub>2</sub>O<sub>3</sub> p-n diodes with the JTE were fabricated. In addition to the static I-V and C-V characteristics, an on-wafer DPT set-up was developed to measure the switching waveforms of the JTE-PND. Under the same measurement set-up, the Ga<sub>2</sub>O<sub>3</sub> JTE-PND shows similar switching speed compared to the commercial SiC SBDs. These

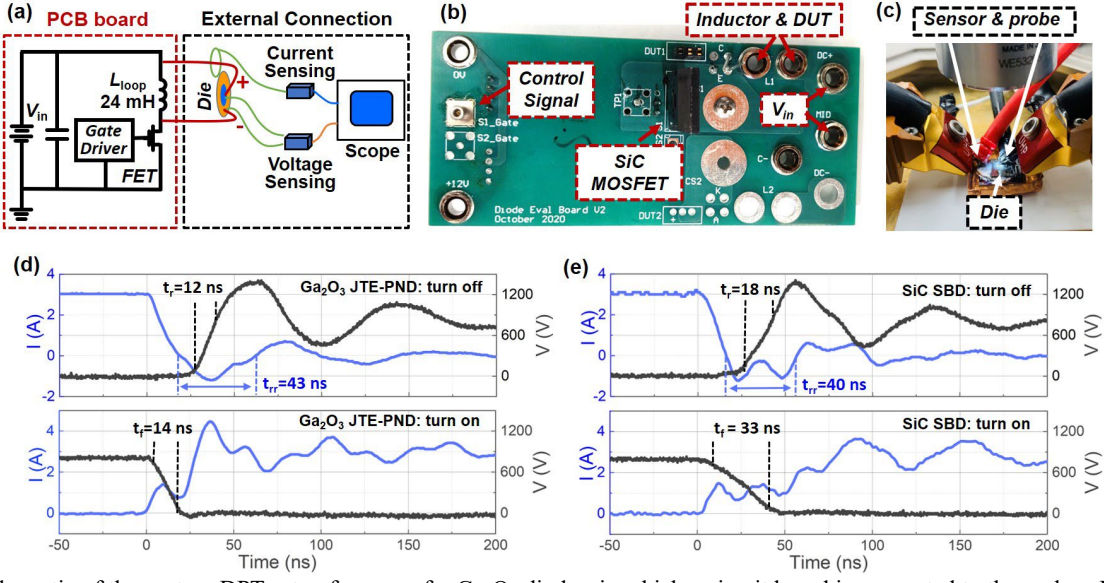


Fig. 6. (a) Schematic of the custom DPT setup for on-wafer  $Ga_2O_3$  diodes, in which a circuit board is connected to the probes. Photos of the (b) test board and (c) the two high-current probes for on-wafer device test. The 800V/3A turn-off and turn-on waveforms of (a)  $Ga_2O_3$  JTE-PNDs and (b) commercial SiC SBDs. The reverse recovery time  $(t_{rr})$  of both diodes are similar. The rise time  $(t_r)$  and fall time  $(t_f)$  of SiC SBDs are higher due to the higher current rating (larger charges) than the  $Ga_2O_3$  JTE-PNDs.

Table I. Comparison of the edge termination technologies for Ga<sub>2</sub>O<sub>3</sub> diodes.

Edge termination	Diode	Ref	Junction field (MV/cm)	JTE Capacitance	Switching metrics	Diff. R <sub>ON,SP</sub> (mΩ·cm²)	BV (V)
Multi-layer NiO JTE	PND	This work	4.2	Low (11% of a ~1A device)	small rise/fall /reverse- recovery time	4	3300
N implant + FP	SBD	[7]	2.45	-	-	4.7	1430
Trench + FP	SBD	[8]	4	-	-	8.8	2890
High-k FP	SBD	[16]	5.45	-	-	0.32	687

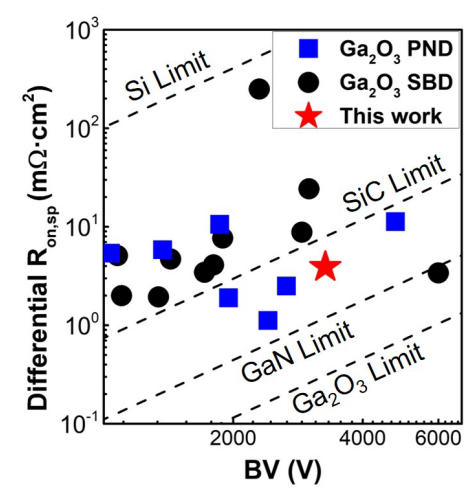


Fig. 7.  $R_{\text{ON,SP}}$  vs. BV benchmark of the fabricated  $Ga_2O_3$  JTE-PND with other  $Ga_2O_3$  power diodes.

results provide useful references for advancing the Ga<sub>2</sub>O<sub>3</sub> devices towards power electronics applications.

## REFERENCES

- [1] Y. Zhang, F. Udrea, and H. Wang, "Multidimensional device architectures for efficient power electronics," *Nat. Electron.*, vol. 5, no. 11, Art. no. 11, Nov. 2022.
- [2] M. Higashiwaki et al., "Recent progress in Ga2O3power devices," Semicond. Sci. Technol., vol. 31, no. 3, p. 034001, Jan. 2016.
- [3] J. A. Spencer et al., "A review of band structure and material properties of transparent conducting and semiconducting oxides: Ga2O3, Al2O3, In2O3, ZnO, SnO2, CdO, NiO, CuO, and Sc2O3," Appl. Phys. Rev., vol. 9, no. 1, p. 011315, Mar. 2022.
- [4] Y. Qin, Z. Wang, K. Sasaki, J. Ye, and Y. Zhang, "Recent progress of Ga2O3 power technology: large-area devices, packaging and applications," *Jpn. J. Appl. Phys.*, vol. 62, no. SF, p. SF0801, Feb. 2023.

- [5] Y. Qin, B. Albano, J. Spencer, J. S. Lundh, B. Wang, C. Buttay, M. Tadjer, C. DiMarino, and Y. Zhang, "Thermal management and packaging of wide and ultra-wide bandgap power devices: a review and perspective," J. Phys. Appl. Phys., vol. 56, no. 9, p. 093001, Feb. 2023.
- [6] N. Allen et al., "Vertical Ga<sub>2</sub>O<sub>3</sub> Schottky Barrier Diodes With Small-Angle Beveled Field Plates: A Baliga's Figure-of-Merit of 0.6 GW/cm<sup>2</sup>," IEEE Electron Device Lett., vol. 40, no. 9, pp. 1399–1402, Sep. 2019.
- [7] C.-H. Lin et al., "Vertical Ga2O3 Schottky Barrier Diodes With Guard Ring Formed by Nitrogen-Ion Implantation," *IEEE Electron Device Lett.*, vol. 40, no. 9, pp. 1487–1490, Sep. 2019.
- [8] W. Li, K. Nomoto, Z. Hu, D. Jena, and H. G. Xing, "Field-Plated Ga2O3 Trench Schottky Barrier Diodes With a BV2/ Ron,sp of up to 0.95 GW/cm2," *IEEE Electron Device Lett.*, vol. 41, no. 1, pp. 107–110, Jan. 2020
- [9] Y. Kokubun, S. Kubo, and S. Nakagomi, "All-oxide p-n heterojunction diodes comprising p-type NiO and n-type β-Ga2O3," *Appl. Phys. Express*, vol. 9, p. 091101, Aug. 2016.
- [10] H. H. Gong et al., "A 1.86-kV double-layered NiO/β-Ga2O3 vertical pn heterojunction diode," Appl. Phys. Lett., vol. 117, no. 2, p. 022104, Jul. 2020.
- [11] Y. Ma et al., "Tri-gate GaN junction HEMT," Appl. Phys. Lett., vol. 117, no. 14, p. 143506, Oct. 2020.
- [12] M. Xiao et al., "First Demonstration of Vertical Superjunction Diode in GaN," in 2022 International Electron Devices Meeting (IEDM), Dec. 2022, p. 35.6.1-35.6.4
- [13] W. Hao, F. Wu, W. Li, G. Xu, X. Xie, K. Zhou, W. Guo, X. Zhou, Q. He, X. Zhao, S. Yang, and S. Long, "High-Performance Vertical β-Ga2 O3 Schottky Barrier Diodes Featuring P-NiO JTE with Adjustable Conductivity," in 2022 International Electron Devices Meeting (IEDM), Dec. 2022, p. 9.5.1-9.5.4.
- [14] B. Wang, et al., "2.5 kV Vertical Ga2O3 Schottky Rectifier With Graded Junction Termination Extension," *IEEE Electron Device Lett.*, vol. 44, no. 2, pp. 221–224, Feb. 2023.
- [15] M. Xiao, et al., "NiO junction termination extension for high-voltage (>3 kV) Ga<sub>2</sub>O<sub>3</sub> devices," Appl. Phys. Lett., under review, Mar. 2023.
- [16] S. Roy, A. Bhattacharyya, P. Ranga, H. Splawn, J. Leach, and S. Krishnamoorthy, "High-k Oxide Field-Plated Vertical (001) β-Ga2O3 Schottky Barrier Diode With Baliga's Figure of Merit Over 1 GW/cm2," *IEEE Electron Device Lett.*, vol. 42, no. 8, pp. 1140–1143, Aug. 2021.